

Exploiting cellophane birefringence to generate radially and azimuthally polarised vector beams

Johnston Kalwe^{1,2}, Martin Neugebauer^{2,3}, Calvin Ominde¹,
Gerd Leuchs^{2,3,4}, Geoffrey Rurimo¹ and Peter Banzer^{2,3,4}

¹Jomo Kenyatta University of Agriculture & Technology, Department of Physics,
PO Box 62000-00200, Nairobi, Kenya

²Max Planck Institute for the Science of Light, Guenther-Scharowsky-Str. 1, D-91058
Erlangen, Germany

³Institute of Optics, Information and Photonics, Department of Physics, Friedrich-
Alexander-University Erlangen-Nuremberg, Staudtstr. 7/B2, D-91058 Erlangen,
Germany

⁴Department of Physics, University of Ottawa, 25 Templeton, Ottawa, Ontario,
K1N 6N5 Canada

E-mail: johnston.kalwe@gmail.com

Received 13 October 2014, revised 12 December 2014

Accepted for publication 8 January 2015

Published 4 February 2015



CrossMark

Abstract

We exploit the birefringence of cellophane to convert a linearly polarised Gaussian beam into either a radially or azimuthally polarised beam. For that, we fabricated a low-cost polarisation mask consisting of four segments of cellophane. The fast axis of each segment is oriented appropriately in order to rotate the polarisation of the incident linearly polarised beam as desired. To ensure the correct operation of the polarisation mask, we tested the polarisation state of the generated beam by measuring the spatial distribution of the Stokes parameters. Such a device is very cost efficient and allows for the generation of cylindrical vector beams of high quality.

Keywords: polarisation mask, cellophane, birefringence, radial, azimuthal

1. Introduction

Cylindrically polarised vector beams have attracted much attention in a wide range of scientific and technological disciplines due to their unique properties and potential applications. For instance, when a beam with radial polarisation is focused using a high numerical aperture system, an intense longitudinal component of the electric field results in the focal region [1].

This longitudinal field has been confirmed in various publications [2–9], and a smaller spot size in comparison to a linearly polarised beam has been reported [2, 3]. Because of those properties, radially polarised beams have found several applications in optical data storage [10] and laser machining [11, 12]. Furthermore, both tightly focused azimuthally and radially polarised light beams have proven to be versatile tools in the field of optical trapping [13, 14], microscopy [15] and nanoplasmonics [16, 17].

This interest in radially and azimuthally polarised beams also fostered the development of many different techniques on how to generate these beams. For instance, a polarisation state with cylindrical symmetry can be prepared inside a laser cavity, for example, by using binary dielectric diffraction gratings or a conical Brewster prism [18, 19]. But, external methods also have been introduced where specially designed polarisation converters, axicon lenses or interferometric arrangements that involve coherent superposition of linearly polarised beams are utilized [1, 20–27]. However, each of these methods has its own drawbacks, especially when considering the cost factor. For example, commercially available liquid crystal-based devices can cost several thousand US dollars.

Here, we describe a simple procedure for fabricating a reliable and cost-effective mode converter. All necessary components can be found in basic laboratories. The concept of our approach has already been reported in various publications, where segmented commercial waveplates (polarisation converters) have been used to rotate the polarisation state locally [28, 29]. In this paper, we further develop this concept with regard to cost efficiency. For that purpose, we use cellophane with fitting birefringence properties to fabricate a polarisation mask for the generation of cylindrical vector beams of high quality, comparable with commercial devices.

2. Design and fabrication of the polarisation mask

The purpose of our device is to convert the homogeneously linear polarisation distribution of an incoming Gaussian beam into the lateral position dependent polarisation distribution of a radially (E_{rad}) or azimuthally polarised beam (E_{azi}) that can be described by [25]

$$\begin{aligned} E_{\text{rad}}(x, y) &= E_0 \left(x e^{-\frac{x^2+y^2}{w^2}} \hat{e}_x + y e^{-\frac{x^2+y^2}{w^2}} \hat{e}_y \right) \\ E_{\text{azi}}(x, y) &= E_0 \left(y e^{-\frac{x^2+y^2}{w^2}} \hat{e}_x - x e^{-\frac{x^2+y^2}{w^2}} \hat{e}_y \right). \end{aligned}$$

The basic principle of the underlying polarisation conversion is depicted in figure 1. An incoming linearly polarised beam passes through a segmented half-waveplate. As in [28, 29], each segment has a differently oriented fast axis. When a linearly polarised Gaussian beam is passed through the polarisation mask, each segment rotates the polarisation of the linearly polarised incident beam into a pseudo-radially or pseudo-azimuthally polarised beam. As shown in figure 1, the polarisation state of the generated beam can be switched from, for instance, radial to azimuthal by simply rotating the polarisation of the linearly polarised incoming beam from vertical to horizontal.

Next, we outline a procedure to build such a device from cellophane. In the first step, cellophane with appropriate birefringence properties is identified and characterized [30–33]. Ideally, it shows the retardation of a half-waveplate. After determining the fast axis of the sheet, four segments with identical shape but differently oriented fast axes (0° , 45° , -45° , 90°) are cut out of the corresponding sheet (see figure 2(a)) using a CO_2 laser engraving/cutting

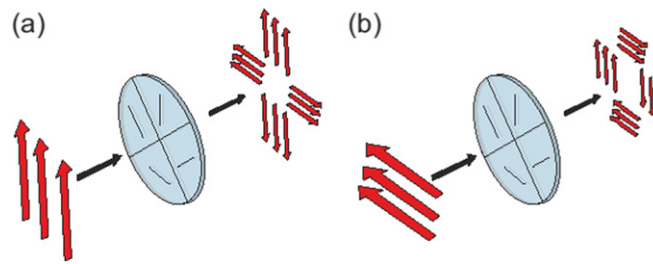


Figure 1. Working principle of a segmented waveplate-based polarization converter. Generation of a (a) (pseudo-)radially or (b) (pseudo-)azimuthally polarized light beam for a vertically or horizontally linearly polarized input beam, respectively.

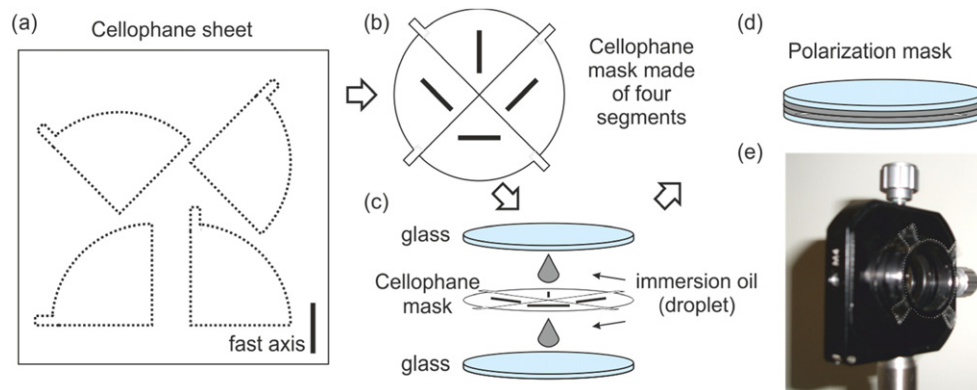


Figure 2. (a) Cutting template for the cellophane. (b) The four cellophane segments assembled to a polarization mask. (c) The polarization mask is fixed between two microscope cover slips (glass) and immersion oil is inserted. (d) Sketch of the fabricated polarization mask and (e) an image of the device mounted on a lens holder.

machine. Alternatively, simple and cheap mechanical methods for cutting the cellophane allow for similar edge quality. Such methods include cutting with scissors or a scalpel. Extensions are included in the cut-outs to aid in joining the four segments together. To complete fabrication of the polarisation mask, we sandwich the four segments between two microscope cover slips (glass) and insert immersion oil matching the refractive index of glass. This approach serves a dual purpose. Because of adhesion forces, the four cellophane segments are fixed between the two cover slips (no additional glue is needed). Furthermore, wavefront aberrations and speckles caused by the surface roughness of the cellophane are reduced. Finally, the performance of our device as a mode and polarisation converter can be tested experimentally.

3. Generation of a radially polarised beam using the polarisation mask

The setup for the conversion of a linearly polarised Gaussian to a radially or azimuthally polarised beam is shown in figure 3(a). The linearly polarised fundamental Gaussian mode of a frequency-stabilized He-Ne laser (wavelength $\lambda = 633$ nm) is spatially filtered, expanded and collimated. Expansion of the beam (full width at half maximum of 4 mm) ensures that it

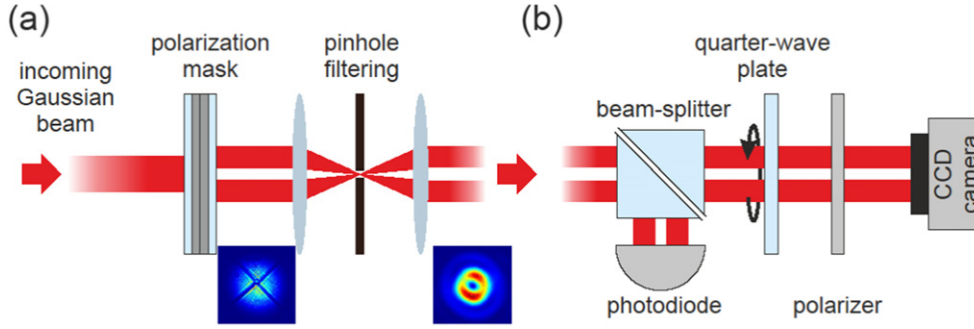


Figure 3. (a) Experimental setup used for the generation of either radially or azimuthally polarized beams. An incoming linearly polarized Gaussian beam passes through the fabricated polarization mask. Pictures in the insets show beam patterns captured at various locations. Spatial filtering with a pinhole results in a radially polarized beam whose mode quality and purity are significantly improved. (b) Setup for measuring the Stokes polarization parameters of the generated doughnut beam. A nonpolarizing beam-splitter guides a fraction of the incoming beam onto a photodiode as a reference signal. The quarter-wave plate is mounted on a rotatable mount while the linear polarizer is fixed. A CCD camera is used to analyse the image patterns.

covers a large portion of the cellophane sheet and thereby minimizes the effect of a nonperfect central area of the fabricated polarisation mask. It is then passed through a linear polarizer, which serves to define its polarisation as either horizontal or vertical. Subsequently, the beam impinges onto the polarisation mask, which converts either a vertically polarised Gaussian beam into a pseudo-radially polarised beam or a horizontally polarised Gaussian beam into a pseudo-azimuthally polarised beam. The segmented polarisation pattern with its sharp edges is not stable under propagation because of diffraction. But the generated beam is a superposition of higher order modes where each by itself is similar, expanding at a different rate under diffraction. To achieve high mode purity of the fundamental cylindrically polarised mode, the higher order modes are filtered out utilizing a spatial filter. The spatial filter comprises two doublet lenses and a pinhole of diameter $30\ \mu\text{m}$ as shown in figure 3(a). With the second lens after the pinhole, the beam is collimated and its spatial structure analysed using a charge-coupled device (CCD) camera.

To quantify the polarisation purity of the generated doughnut beam, we measure the Stokes parameters,

$$S_0 = |E_x|^2 + |E_y|^2, S_1 = |E_x|^2 - |E_y|^2, S_2 = E_x E_y \cos \varphi, S_3 = E_x E_y \sin \varphi,$$

spatially resolved. S_0 represents the total intensity, while S_1 and S_2 describe the linear polarisation in the horizontal-vertical basis and in the diagonal-antidiagonal basis, respectively. S_3 quantifies the amount of circular polarisation [27, 34, 35]. In the experiment, the Stokes parameters are measured by using the rotating quarter-waveplate technique (setup shown in figure 3(b)) [35]. The output beam is passed through a rotatable quarter-waveplate and a fixed linear polarizer. Behind the polarizer, a CCD camera is used to measure the beam profile for different angular positions of the quarter-waveplate. Using the algorithm

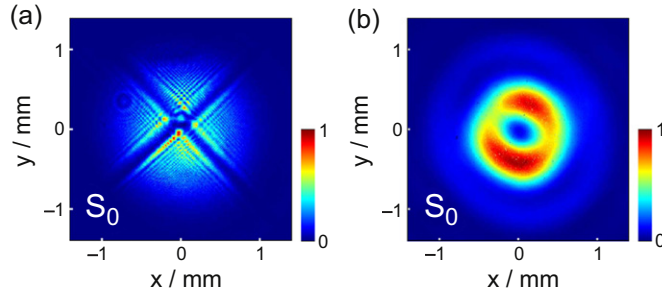


Figure 4. (a) Intensity profile of an incoming linearly polarized light beam immediately after passing through the polarization mask. (b) The high-quality vector beam obtained after spatial filtering. There should be no azimuthal dependence of the intensity around the ring. Instead, a variation by 50% is observed (see text for details). Both beam profiles are demagnified by a factor of four in order to fit the dimensions of the camera chip.

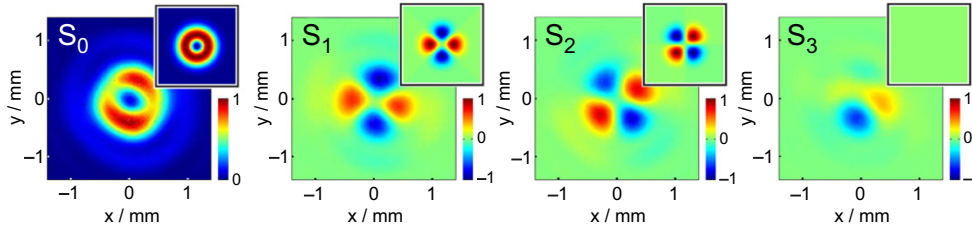


Figure 5. Experimentally measured and calculated (see insets) distributions of the spatially resolved Stokes parameters S_0 , S_1 , S_2 and S_3 of a radially polarized beam. All Stokes parameters are normalized to the maximum value of S_0 .

introduced in [35], the spatially resolved Stokes parameters are reconstructed from sixteen different images of the beam.

4. Experimental results and discussion

Figure 4(a) shows the intensity distribution S_0 of the generated beam emerging from the polarisation mask measured directly behind the mask before the spatial filtering. For demonstration purposes, we choose the incoming beam to be vertically polarised.

The pseudo-radially polarised beam obtained immediately after the polarisation mask has a poor mode quality (see figure 4(a)). This is due to the fact that the mask with the cellophane segments introduces abrupt changes in the transverse beam properties and the impinging light beam is scattered and diffracted at these edges. In addition, the limited number of segments, as well as the mediocre overlap between the intensity distributions of the incoming and the desired beam, results in the generation of higher order modes [29]. When introducing the aforementioned pinhole filtering, the quality of the generated mode can be increased significantly (see figure 4(b)). Alternatively, the mode purity can be improved by letting the beam emerging from the mask propagate for several metres. Due to the fact that higher order modes diffract more rapidly, the central part of the beam close to the optical axis purifies. In

this even more cost-efficient manner, simple aperture is sufficient to filter the lowest order doughnut-shaped part of the beam.

Figure 5 shows the spatial distribution of the experimentally obtained normalized Stokes parameters S_0 , S_1 , S_2 and S_3 of the filtered radially polarised beam, with the insets illustrating the theoretically expected distributions. Considering the intensity profile of the beam, the typical ring-like distribution of the S_0 parameter can be seen. The small deviations from the theoretical intensity distribution are caused by residual higher order modes, which are not filtered out by the pinhole. Additionally, lower intensity circular polarisation components can be seen, although S_3 should be exactly zero everywhere in the plane of observation. This deviation is likewise attributed to small imperfections of the mask introduced by the relative alignment of the segments and their position relative to the incoming beam, the remaining roughness of the edges of the segments, etc. The linear polarisation distributions S_1 and S_2 , however, show a very good overlap with the respective theoretical prediction, clearly indicating the generation of a good quality radially polarised beam.

In order to put the discussion of the mode quality into perspective, a short consideration of the actual costs of our device seems appropriate. We used two microscope cover slips (0.3 US dollar), two droplets of immersion oil (0.1 US dollar), and roughly 10 mm² of cellophane (1 m² costs about 0.3 US dollar) for the polarisation mask. Even though we had to test larger areas of different cellophane sheets to find one with the desired birefringence properties, the actual cost for building a single device is below 1 US dollar.

5. Conclusion

We have demonstrated that beams with either radial or azimuthal polarisation can be generated from a linearly polarised beam using our cellophane-based polarisation mask. Such a polarisation mask consists of four (or more) segments, each with different orientation of the fast axis. Our masks are easy to fabricate, and the use of cellophane makes this technique easily achievable and highly cost effective. To improve the mode, a pinhole (spatial) filter was used to filter out higher order modes while preserving the radial or azimuthal polarisation components. In future work, the number of segments of the polarisation mask can be increased to enhance the mode overlap of the incoming and the desired beam [29]. Furthermore, more complex polarisation masks can be designed producing different types of polarisation patterns.

Acknowledgments

We thank Uwe Mick for support during the cutting of cellophane segments. Further, one of the authors (JD) is grateful to Deutscher Akademischer Austausch Dienst for the support during this work.

References

- [1] Scully M and Zubairy M 1991 Simple laser accelerator: optics and particle dynamics *Phys. Rev. A* **44** 2656–63
- [2] Quabis S, Dorn R, Eberler M, Glöckl O and Leuchs G 2000 Focusing light to a tighter spot *Opt. Commun.* **179** 1–7
- [3] Dorn R, Quabis S and Leuchs G 2003 Sharper focus for radially polarised light beam *Phys. Rev. Lett.* **91** 233901

- [4] Youngworth K S and Brown T G 2000 Focusing of high numerical aperture cylindrical-vector beams *Opt. Express* **7** 77–87
- [5] Biss D and Brown T 2001 Cylindrical vector beam focusing through a dielectric interface *Opt. Express* **9** 490–6
- [6] Quabis S, Dorn R, Eberler M, Glöckl O and Leuchs G 2001 The focus of light—theoretical calculation and experimental tomographic reconstruction *Appl. Phys. B* **72** 109–13
- [7] Miyaji G, Miyanaga N, Koji T, Sueda K and Ken O 2004 Intense longitudinal electric fields generated from transverse electromagnetic waves *Appl. Phys. Lett.* **84** 3855–7
- [8] Pereira S F and van de Nes A S 2004 Superresolution by means of polarisation, phase and amplitude pupil masks *Opt. Commun.* **234** 119–24
- [9] Rurimo G K *et al* 2006 Using a quantum well heterostructure to study the longitudinal and transverse electric field components of a strongly focused laser beam *J. Appl. Phys.* **100** 1–6
- [10] Li X, Cao Y and Gu M 2011 Superresolution-focal-volume induced 3.0 Tbytes/disk capacity by focusing a radially polarized beam *Opt. Lett.* **36** 2510–2
- [11] Niziev V and Nesterov V 1999 Influence of beam polarization on laser cutting efficiency *J. Phys. D* **32** 1455–61
- [12] Krishnan V and Tan B 2012 Generation of radially polarized beam for laser micromachining *J. Laser Micro/Nanoengineering* **7** 274–8
- [13] Zhan Q 2004 Trapping metallic Rayleigh particles with radial polarization *Opt. Express* **12** 3377–82
- [14] Kozawa Y and Sato S 2010 Optical trapping of micrometer-sized dielectric particles by cylindrical vector beams *J. Opt.* **18** 10828–33
- [15] Hao X, Kuang C, Wang T and Liu X 2010 Effects of polarization on the de-excitation dark focal spot in STED microscopy *J. Opt.* **12** 115707
- [16] Kindler J, Banzer P, Quabis S, Peschel U and Leuchs G 2007 Waveguide properties of single subwavelength holes demonstrated with radially and azimuthally polarized light *Appl. Phys. B* **89** 517–20
- [17] Sancho-Parramon J and Bosch S 2012 Dark modes and fano resonances in plasmonic clusters excited by cylindrical vector beams *ACS Nano* **6** 8415–23
- [18] Moser T, Balmer J, Delbeke D, Muys P, Verstuyft S and Baets R 2006 Intracavity generation of radially polarized CO₂ laser beams based on a simple binary dielectric diffraction grating *Appl. Opt.* **45** 8517–20
- [19] Kozawa Y and Sato S 2005 Generation of a radially polarized laser beam by use of a conical Brewster prism *Opt. Lett.* **30** 3063–5
- [20] Tidwell S, Ford D and Kimura W 1990 Generating radially polarized beams interferometrically *Appl. Opt.* **29** 2234–9
- [21] Stalder M and Schadt M 1996 Linearly polarized light with axial symmetry generated by liquid-crystal polarization converters *Opt. Lett.* **21** 1948–50
- [22] Oron R, Shmuel B, Davidson N and Asher A 2000 The formation of laser beams with pure azimuthal or radial polarization *Appl. Phys. Lett.* **77** 3322–4
- [23] Neil M A A, Massoumian F, Juskaitis R and Wilson T 2002 Method for the generation of arbitrary complex vector wave fronts *Opt. Lett.* **27** 1929–31
- [24] Passilly N, Denis R and Kamel A 2005 Simple interferometric technique for generation of a radially polarized light beam *J. Opt. Soc. Am. A* **22** 984–91
- [25] Zhan Q 2009 Cylindrical vector beams: from mathematical concepts to applications *Adv. Opt. Photonics* **1** 1–57
- [26] Maurer C, Jesacher A, Fürhapter S, Bernet S and Ritsch-Marte M 2007 Tailoring of arbitrary optical vector beams *New J. Phys.* **9** 78
- [27] Ramirez-Sanchez V, Piquero G and Santarsiero M 2009 Generation and characterization of spirally polarized fields *J. Opt. A: Pure Appl. Opt.* **11** 1–6
- [28] Maekawa A and Uesaka M 2008 Generation of radial polarized laser beam and its applications for accelerator *Proc. FEL08* **8** 435–8
- [29] Quabis S, Dorn R and Leuchs G 2005 Generation of a radially polarized doughnut mode of high quality *Appl. Phys. B* **81** 597–600
- [30] Ortiz-Gutierrez M, Olivares-Peres A and Sanchez V 2001 Cellophane film as half wave retarder of wide spectrum *Opt. Mater.* **17** 395–400
- [31] Iizuka K 2003 Cellophane as a half-wave plate and its use for converting a laptop computer screen into a 3D display *Rev. Sci. Instrum.* **74** 3636–9

- [32] Iizuka K 2012 Complementary cellophane optic gate and its use for a 3D iPad without glass *Rev. Sci. Instrum.* **83** 043710
- [33] Kinyua D M, Rurimo G K, Karimi P K, Maina S N and Ominde F C 2013 Interferometry analysis of cellophane birefringence *Opt. Photonics J.* **3** 337–41
- [34] Martinez-Herrero R, Mejias P M and Piquero G 2009 *Characterization of Partially Polarized Light Fields* (Berlin: Springer)
- [35] Schaefer B, Collet E, Smyth R, Barret D and Fraher B 2007 Measuring the stokes polarization parameters *Am. J. Phys.* **75** 163–8